

Title: OPERATION OF THE HIGH BRIGHTNESS LINAC FOR
THE ADVANCED FREE-ELECTRON LASER INITIATIVE
AT LOS ALAMOS

5-184

Author(s): Richard L. Sheffield, R. H. Austin, K. C. D. Chan, S. M.
Gierman, J. M. Kinross-Wright, S. H. Kong, D. C. Nguyen,
S. J. Russell, and C. A. Timmer

Submitted to: 1993 Particle Accelerator Conference
Washington, DC
May 17-20, 1993

DISCLAIMER

This report was prepared as an account of work sponsored by an agency of the United States Government. Neither the United States Government nor any agency thereof, nor any of their employees, makes any warranty, express or implied, or assumes any legal liability or responsibility for the accuracy, completeness, or usefulness of any information, apparatus, product, or process disclosed, or represents that its use would not infringe privately owned rights. Reference herein to any specific commercial product, process, or service by trade name, trademark, manufacturer, or otherwise does not necessarily constitute or imply its endorsement, recommendation, or favoring by the United States Government or any agency thereof. The views and opinions of authors expressed herein do not necessarily state or reflect those of the

Los Alamos
NATIONAL LABORATORY

Los Alamos National Laboratory, an affirmative action/equal opportunity employer, is operated by the University of California for the U.S. Department of Energy under contract W-7405-ENG-30. By acceptance of this article, the publisher recognizes that the U.S. Government retains a nonexclusive, royalty-free license to publish or reproduce the published form of this contribution, or to allow others to do so, for U.S. Government purposes. The Los Alamos National Laboratory requests that the publisher identify this article as work performed under the auspices of the U.S. Department of Energy.

Operation of the High Brightness LINAC for the Advanced Free-Electron Laser Initiative at Los Alamos*

R. L. Sheffield, R. H. Austin, K. D. Chan, S. M. Gierman, J. M. Kinross-Wright, S. H. Kong,
D. C. Nguyen, S. J. Russell, and C. A. Timmer
Los Alamos National Laboratory
Los Alamos, NM 87545

Abstract

Free-electron lasers and high energy physics accelerators have increased the demand for very high-brightness beam sources. This paper describes the design of an accelerator which has produced beams of less than 2.1π mm-mrad at 1 nC and emittances of 3.7 and 6.5π mm-mrad for 2 and 3 nC, respectively. The accelerator has been operated between 10 and 18 MeV. The beam emittance growth in the accelerator is minimized by using a photoinjector electron source integrated into the design of the linac, a focusing solenoid to correct the emittance growth caused by space charge, and a special design of the coupling slots between accelerator cavities to minimize quadrupole effects.

Introduction

A new accelerator design that produces a very bright electron beam in a compact form has been constructed through the Advanced Free-Electron Laser Initiative (AFEELI) [1] at Los Alamos National Laboratory. State-of-the-art components were incorporated so that the FEL system will be compact, robust, and user friendly.

The design goals for the accelerator are greater 2 nC charge per micropulse and an effective emittance of less than 5π mm-mrad. Simple design is accomplished by using a single radio-frequency feed to drive the entire accelerator structure. The accelerator (Fig. 1) design has the following features: maximum 20-MeV output energy, maximum average cell gradients of 22 MeV/m, up to 100-Hz repetition rate, up to 30- μ s long macropulses, 8- to 20-ps long micropulses, and liquid-nitrogen operation capability. The accelerator operates with a 1300-MHz, 17-MW-peak-power klystron [1].

Simulations

The following definition is used for the normalized rms emittance for the simulations,

$$\epsilon_n = \beta \gamma r_x = \pi \beta \gamma [\langle x^2 \rangle \langle x'^2 \rangle - \langle x x' \rangle^2]^{1/2},$$

where γ is the relativistic factor, β is the particle velocity, divided by the speed of light, x is the transverse beam size, x' is the transverse beam divergence, and r_x is the unnormalized emittance. The emittance is calculated in two ways. The "full" emittance is calculated by using the entire micropulse in time and space.

*Work supported by Los Alamos National Laboratory Institutional Supporting Research, under the auspices of the United States Department of Energy

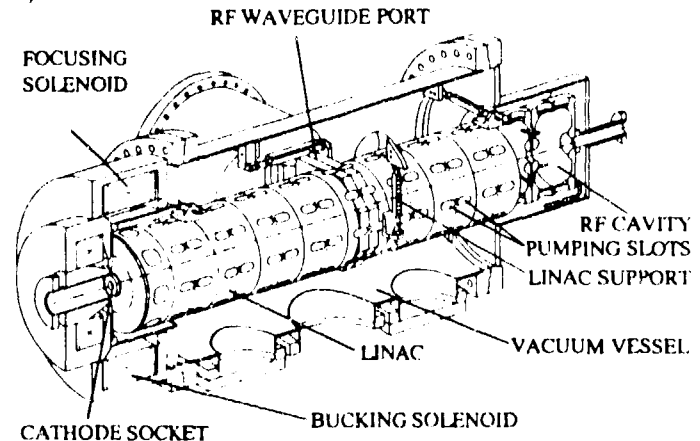


Figure 1. AFEEL linac schematic. The focusing solenoid provides compensation of space-charged induced emittance growth. The Bucking Solenoid is adjusted to give zero field at the surface of the cathode. The LINAC is an eleven-cell pi-mode structure. The LINAC can be operated down to 77K. The support structures allow only rotation of the accelerator on cool-down, not translation.

The "slice" emittance is calculated by dividing a micropulse into slices in time equal to a slippage length. To ensure enough particles are in a slice to give reasonable statistics, the smallest time slice is limited to 1% of the total pulse length (4000 particles were used in the simulations). We calculate the slice emittance because the electrons are not matched to the wiggler over the entire pulse, but only for the middle portion (in time) of the pulse. Because temporal mixing can occur downstream of the accelerator, the use of slice emittance is only valid at the location of the wiggler.

Emittance Compensation

Surrounding the first few cells is a large focusing solenoid. The use of a solenoid to correct emittance growth caused by space charge has been discussed in detail in several papers.[2] A brief explanation of emittance compensation follows. As an electron bunch leaves the cathode, the bunch expands radially because of radial space charge forces. Since the space charge force acts continuously on the bunch, no single discrete lens can compensate for the distortion of the distribution in phase space. However, a simple lens can be used to focus the bunch. Then, to the first order, the same forces that acted on the bunch during expansion are present while the bunch is focused. Thus, the emittance growth that has occurred can be significantly reduced by proper lens placement. To accurately render the solenoid field profiles, we incorporated the POISSON field maps of the solenoid directly into a modified version PARMELA.

Coupling Slot Arrangement

The standing-wave, 1300-MHz, π -mode accelerator is designed with on-axis coupling slots [2]. By incorporating MAFIA field maps of the coupling slots into PARMELA, we found that coupling cells with only two-coupling-slots produced a quadrupole lens in every accelerator cell. Therefore, it was necessary to change the coupling slot geometries to eliminate asymmetric focusing in the accelerator.

The effect of coupling slots is significant for very high-brightness beams. A single slot produces a dipole lens, two slots produce a quadrupole lens, four slots produces an octupole lens, and so on. Each accelerator cell (except the cells at the accelerator ends) has coupling slots on each half of an accelerator cell. The relative orientation of the slots on either end of the cell will determine the relative angle of the corresponding lens. The two-coupling-slot configuration gives a quadrupole lens at the entrance and exit of the accelerator cell. The orientation of the slots will determine whether the quadrupole lens add or subtract focusing for each cell. Thus, the coupling cells can be configured such that the fields at each cell end cancel, giving a net effect close to zero for a relativistic beam.

The coupling-slot design for the AFEL accelerator uses a four-coupling-slot arrangement for the first two cells. Because the four-slot arrangement has no quadrupole component, then the first two cells produce no beam asymmetry. The four-coupling-slot arrangement cannot be carried throughout the accelerator. At high currents a dipole mode will build up which is easily coupled through a four-coupling-slot cell and causes beam-breakup for more than two cells. After the beam exits the first two cells, the beam is relativistic, and the remaining cells have a two-coupling-slot arrangement that gives a very small net quadrupole focusing.

Other Design Features

The first cell, a half-cell, is 9 mm longer than one-half of a standard 1300-MHz cell. A longer injection cell has two advantages. First, the exit phase of the electron bunch depends on the cell length. Since the AFEL linac has a single rf feed, the proper operating phase to minimize energy spread was met by adjusting the first cell length. Second, a longer first cell increases the electron-beam energy at the exit of the first cell. This reduces the space charge effects and helps improve the final emittance. The exit energy from the first cell is 1.5 MeV instead of 1.0 MeV for a regular half-cell.

Other engineering features of the AFEL accelerator are the capability of operation at 77K; UHV design; and high Q, high gradient, long macropulse accelerator cells.

Beam Dependencies

This type of accelerator is unique in that the electron beam distribution does not mix longitudinally. With no mixing, the rms emittance calculation for the full pulse overestimates the beam emittance. Except for statistical noise caused by the limited number of particles in the simulation, the slice emittance is time independent during the micropulse. However, the emittance of

the full pulse is significantly larger. The larger full-pulse emittance is caused from the variation in divergence throughout the micropulse.

The AFEL is designed to minimize components and distances and to increase reliability and ease of use. However, the stability of accelerator operation does depend strongly on a few parameters. The parameters that must be tightly controlled are the radius of the cathode; the magnitude of the solenoid field around the cathode region; the accelerator phase; and the magnitude of the accelerator fields.

Operation of the Accelerator

The electron source is a CsK₂Sb photocathode. The accelerator pressure is maintained at 8×10^{-10} Torr. The beamline directly downstream of the accelerator is at 2×10^{-8} . Because of contaminants produced during operation of the rf, the useful operational lifetime of a single cathode, for a minimum 1 nC, is limited to, at most, 2 days. The accelerator has six cathodes available in a cartridge type system. Thus, the cathode cartridge system was refreshed every two weeks. Typical time to replace a cartridge pack was 15 minutes. After replacement, a 4 to 5 hour bake degassed the components exposed to air (typically done during the night).

The drive laser was Nd:YLF. The oscillator produces 50 ps micropulses at 108 MHz. The pulses are then compressed with a grating pair and a fiber-optic line to 8 ps. After compression, two double-pass YLF amplifiers are used to increase the micropulse energy to 20 microjoules. A Pockels Cell is used to obtain macropulses which ranged from a few micropulses to 10 microseconds. A KTP crystal is then used to double the wavelength to 530 nm. -parameters? The gaussian spatial profile of the laser beam is sent through an iris that just lets the middle 1/3 of the light pass. This approximately uniform spatial profile is then imaged onto photocathode.

The accelerator was initially conditioned for operation from 9 to 16 MeV. Since this initial conditioning, the maximum energy has been extended to 18 MeV through the course of normal operation. However, earlier this year, after a year of operation, the accelerator has begun to multipactor. This has limited the minimum beam energy to 14 MeV. However, the EFEL requires an electron energy between 15 to 16.5 MeV, and so cleaning the accelerator to eliminate the multipactoring will be done at later date.

Experimental results

The emittance measurements were taken at an electron beam energy of 13 MeV. A quadrupole is positioned 30 cm upstream from an OTR screen. The FWHM of the electron beam was measured as a function of the quadrupole field strength. The 1 nC data set is shown in Fig. 2. Similar sets were obtained for 2 and 4 nC micropulse charges.

The electron beam produced by this accelerator is characterized by a bright temporal core with high divergence wings at the front and back of the pulse. Very little charge is present in these wings, but, due to the large divergence, the wings significantly increase the rms emittance of the beam. Because of

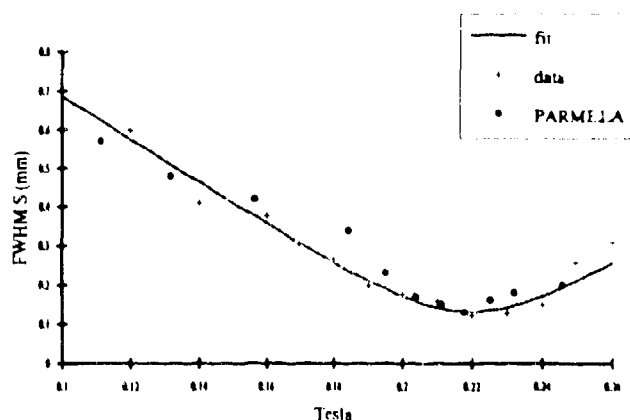


Figure 2. Experimental and simulation data for 1 nC emittance measurement. The simulation data has statistical uncertainty due to the finite number of particles and the distribution of simulation points into bins. The solid curve is a fit to a quadrupole scan function that gives the beam emittance and other beam characteristics.

the small amount of charge, the wings are too tenuous to be observed in the experimental data.

The only means to characterize the performance of the accelerator is to also simulate the quadrupole scan with PARMELA, and then compare the experimental observable - the beam's FWHM size. Figure 3 compares the full rms emittance with the slice emittance and the emittance as calculated by using the FWHM. The emittance as calculated from the FWHM is very close to the slice emittance (the emittance used by the FEL).

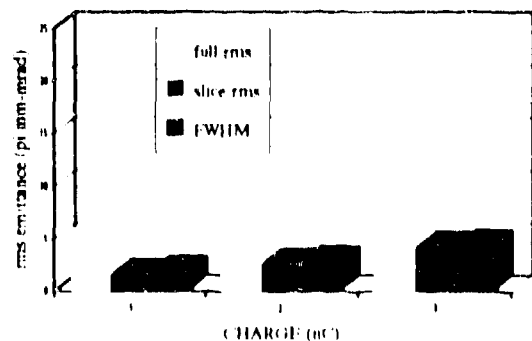


Figure 3. Comparison of PARMELA emittances calculated for the whole beam (full rms), for the rms emittance of a slice (slice rms), and for the FWHM measured from the plot of beam particle number versus transverse dimension (FWHM).

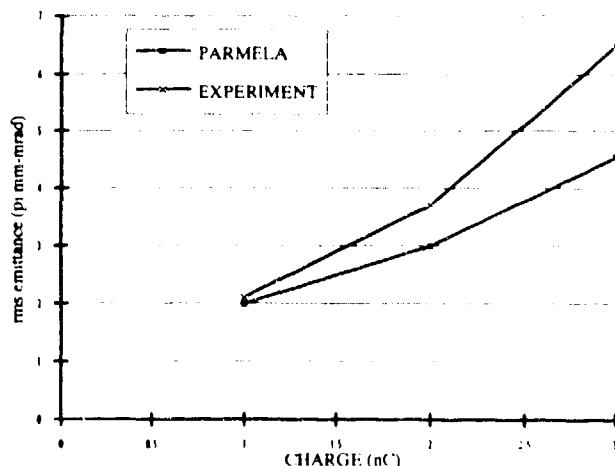


Figure 4. Comparison of experimental and simulation results for several charges.

The FWHM simulation results for the 1 nC case is given in Fig. 2. The agreement between the experiment and simulation is good, indicating that the accelerator is performing as designed for 1 nC.

The emittances for 1, 2, and 3 nC are in Fig. 4. As stated earlier, the agreement is good for 1 nC. However, as the charge is increased the experimental emittance is larger than expected. We have not explored the reason for the increase.

Summary

At 1 nC, the emittance of 2.1π mm-mrad is in good agreement with PARMELA simulation. The measured emittances for 2 and 3 nC are 3.7 and 6.5π mm-mrad, respectively.

References

- [1] K. C. D. Chan, R. H. Kraus, J. Ledford, K. L. Meier, R. E. Meyer, D. Nguyen, R. L. Sheffield, F. E. Sigler, L. M. Young, L. S. Wang, W. L. Wilson, and R. L. Wood, Nucl. Inst. Meth. in Phys., **A318**, 148 (1992)
- [2] B. E. Carlsten, Proc. 10th Int. FEL Conf., Jerusalem, Israel, 1988, Nucl. Instr. and Meth., **A285** (1989) 313; B. E. Carlsten and R. L. Sheffield, Proc. 1988 Linac Conf., Williamsburg, Va., 1988, CERN Report 89-001 (1989) 365; B. E. Carlsten, Proc. 1989 IEEE Part. Accel. Conf., Chicago, IL, IEEE Catalog no. 89CH2669-0 (1989) 313